Semicond. Sci. Technol. **11** (1996) 1569–1574. Printed in the UK

High spatial resolution spectroscopy of single semiconductor nanostructures

T D Harris, D Gershoni, L Pfeiffer, M Nirmal, J K Trautman and J J Macklin

Lucent Technologies, Bell Laboratories, Murray Hill, NJ 07974, USA

Abstract. Low-temperature near-field scanning optical microscopy is used for the first time in spectroscopic studies of single, nanometre dimension, cleaved edge overgrown quantum wires. A direct experimental comparison between a two-dimensional system and a single genuinely one-dimensional quantum wire system, inaccessible to conventional far-field optical spectroscopy, is enabled by the enhanced spatial resolution. We show that the photoluminescence of a single quantum wire is easily distinguished from that of the surrounding quantum well. Emission from localized centres is shown to dominate the photoluminescence from both wires and wells at low temperatures. A factor of three oscillator strength enhancement for these wires compared with the wells is concluded from the photoluminescence excitation data. We also report room-temperature spectroscopy and dynamics of single CdSe nanocrystals. Photochemistry, trap dynamics and spectroscopy are easily determined.

1. Introduction

Modern epitaxial growth techniques allow thickness control of one molecular layer. This dimensional precision has enabled a wide variety of fundamental and applied physics studies. Optoelectronics based on very thin layers of semiconductor heterostructures, such as quantum wells (QWs), in which carriers are confined to two dimensions (2D), are now dominant for many commercial applications. In an attempt to gain further from the reduction of dimensionality, a world-wide research effort to bring 1D quantum structures such as quantum wires (QWRs) and 0D quantum structures such as quantum dots to the same degree of perfection achieved in the 2D quantum systems has been under way during the last decade [1]. The principal barrier to progress is achievement of adequate uniformity in the second- or third-dimensional confinements. While there is no substitute for dimensional uniformity, we show that restriction of the measurements to single quantum wires or single quantum dots permits understanding of the quantum physics not possible for study of ensembles. We discuss in turn low-temperature near-field scanning optical microscopy, (NSOM) of single GaAs quantum wires, and room-temperature confocal scanning optical microscopy of chemically synthesized CdSe quantum dots.

2. Single GaAs quantum wires

Among the most promising ways to achieve dimensional uniformity in 1D structures is cleaved edge overgrowth (CEO) [2]. This technique utilizes two orthogonal directions of epitaxial growth, exploiting the precision of layer thickness control to form uniform intersecting planes of semiconductor. Two different CEO quantum wire systems have been fabricated and studied:

(i) Strained layer QWRs (SQWRs) in which confinement to 1D is produced by one-dimensional pseudomorphic strain [3]. This strain is induced in the (110)-oriented cleaved edge QW by a (100)-oriented strained layer QW.

(ii) T-shaped QWRs (TQWRs) in which quantum confinement to 1D is produced along the intersection line between the planes of a (100)-oriented QW and that of a (110)-oriented cleaved edge overgrown QW [4]. The lateral dimensions of single QWRs produced by this technique are somewhat uncertain, but comparable to the dimensions of the intersecting QW layers from which they are formed.

Since both wire structures are formed by perturbation of quantum wells, these wires are surrounded by the QW from which they are formed. Study of single CEO QWRs requires care to ensure the unambiguous separation of wire and well spectroscopy. Far-field optical spectroscopy, which has been the most common tool for the characterization of 2D structures, suffers a substantial obstacle [5]. The probed volume of a QW is orders of magnitude larger than the probed volume of a QWR. The QWR spectral features are probably obscured by or attributed to QW features. We show here that the enhanced spatial resolution of low-temperature near-field scanning optical microscopy (LT-NSOM) surmounts this obstacle, permitting unambiguous single QWR studies. There is substantial existing

0268-1242/96/111569+06$19.50

spectroscopic data on multiple and arrays of CEO QWRs [3, 4, 6–8]. The added clarity of probing a single wire structure is considerable, since heterogeneity and carrier and electromagnetic field interactions between neighbouring wires are eliminated. We report here low-temperature near-field imaging spectroscopy of the first CEO system, SQWRs.

3. Experiment

The low-temperature NSOM microscope used for this study is described in detail elsewhere [9]. This system was used previously for studies of multiple 'T' quantum wires. We describe here only modifications made to the system in order to allow simultaneous excitation and collection in the near field, required for the study of single wires [10]. All the data reported here used excitation and collection with the same aluminium-coated, tapered fibre probe at a sample temperature of 4 K. The excitation radiation was launched to the fibre from a computer-controlled Ti:sapphire laser. To minimize both mode and amplitude intensity fluctuations and permit polarization control, an intensity stabilizer ('noise eater') and quarter- and half-wave plates were inserted between two separate sections of the Corning 850 nm single-mode fibre used for our NSOM probes. Fusion spliced into the second section of the fibre is a 3dB two-way splitter. It provides a convenient means of simultaneously monitoring the light sent to the probe, and detecting the light collected by the probe. In order to excite and detect through the same tip, efficient discrimination between excitation and emitted light is required. Elastically scattered light is efficiently filtered by a triple spectrometer. The fibre used in this study had no significant fibre fluorescence for the relevant excitation wavelength (700–800 nm). We thus attribute the background light to Raman scattering within the fibre itself. This background light is highly structured and typically one to two orders of magnitude larger than the photoluminescence (PL) signal collected by the tip (diameter $>$ 200 nm) and strongly polarized parallel to the exciting radiation. By careful adjustment of retardation plates in both the excitation and detection channels, extinction ratios of sample luminescence to background of as much as three orders of magnitude could be achieved. This extinction was stable in time and it allows for reliable discrimination against the background. The light emitted around the fibre tip was collected by a reflecting objective contained within the cryostat. The collimated light from this objective was directed to a second monochromator equipped with a CCD camera, allowing simultaneous monitoring of the entire emission spectrum from the sample in both the near and far fields.

The CEO sample used for this study is schematically described in figure 1. In the first growth step, molecular beam epitaxy (MBE) was used to grow five strained $In_{0.10}Ga_{0.90}As$ QWs of 300, 150, 75, 38 and 18 Å respectively, on a (100)-oriented GaAs substrate. The strained QWs, are separated by 1.0 μm thick layers of GaAs and capped by a 2 μm thick GaAs layer. The sample was then thinned, scribed and mounted in a second

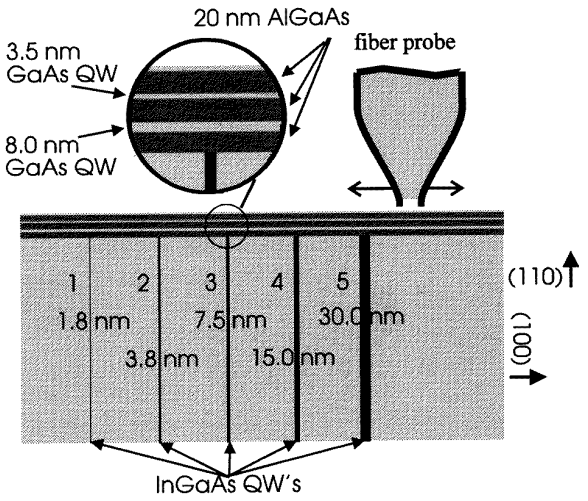

Figure 1. Schematic diagram of the CEO sample structure. The (100) InGaAs QW separation is 1.0 μm, with the fibre tip drawn to this scale to illustrate the expected resolution.

MBE machine. It was cleaved during growth, thus exposing a (110)-facet, onto which the following layers were grown in succession: 200 Å $Al_{0.3}Ga_{0.7}As$, 80 Å, GaAs, 200 Å $Al_{0.3}Ga_{0.7}As$, 35 Å GaAs, 200 Å $Al_{0.3}Ga_{0.7}As$ and 50 Å GaAs. On the original substrate (110) face are thus formed 10 single SQWRs, one wire in each of two (110) QWs, for each of the five (100) strained InGaAs QWs. Low-temperature cathodoluminescence (CL) was used previously to show that emission from the AlGaAs/GaAs (110) QWs is red shifted directly above the strained layers. Here, using NSOM spectroscopy, we overcome two major disadvantages of CL: (i) the loss of spatial resolution due to the large diffusion length ($\sim$1 μm) of the high excess energy cathodo-excited carriers and (ii) the lack of excitation energy tunability.

Two modes of data acquisition were used: PL spectral images are generated by fixing the excitation energy and recording a PL spectrum for 1–5 s at each tip position. A large four-dimensional (x, y, λ, I) data set is thus generated. Alternatively, at a single tip position (image pixel $-x$, y), emission intensity integrated over a selected spectral range is recorded as a function of the excitation energy.

4. Results

In figure 2(a). we show four PL spectra which were selected from the 441 near-field spectra generated in a 21 $\times$ 21 pixel scan of a 2.5 $\times$ 2.5 μm square region of the CEO SQWR sample. The spectra are vertically displaced for clarity. In each spectrum a sharp spectral line is observed. These lines arise from carrier recombination within the (100)-oriented strained InGaAs QWs. The spectrum marked '1' results from recombination in the 18 Å strained QW and the lines marked 2, 3 and 4 result from recombination within the 38, 75 and 150 Å strained QWs respectively. The PL line from the 300 Å strained QW is

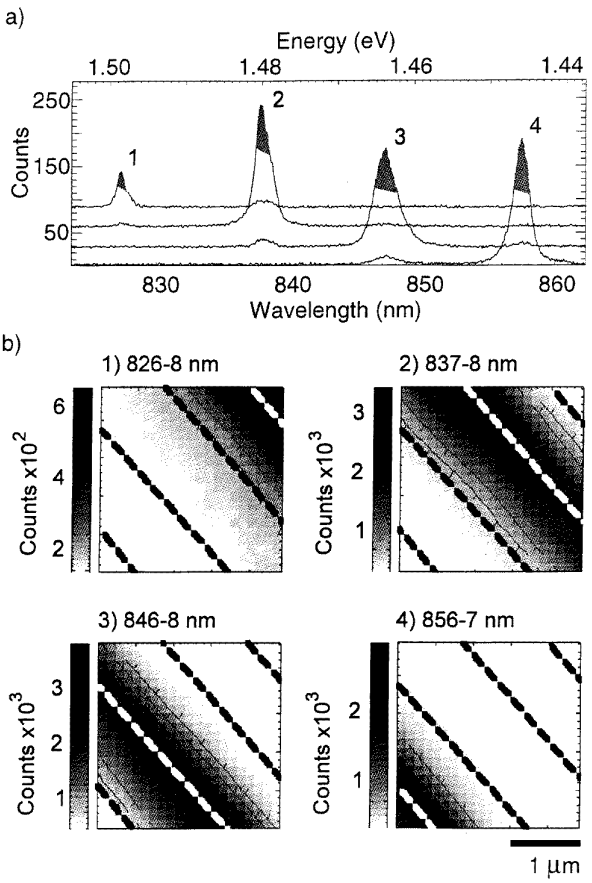

Figure 2. (*a*) Single-pixel PL spectra from an NSOM image. If the emission intensity is integrated over the shaded wavelength interval the four fixed wavelength emission images shown in (*b*) result. Images are numbered from the spectra indicating the wavelength interval. Broken lines are drawn to mark the position of the InGaAs strained QWs and transferred to figure 3(*b*).

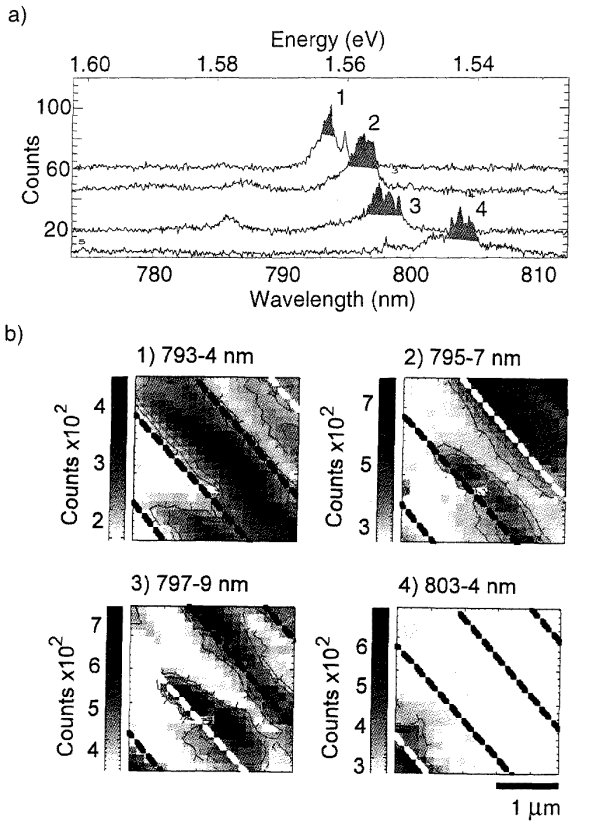

Figure 3. (*a*) Single-pixel PL spectra from the same area as figure 2(*b*) for a wavelength near the 80 Å (110) QW. (*b*) Fixed-wavelength images for the shaded intervals shown above.

not seen in figure 2 since this QW was outside the spatial range of this image.

In figure 2(*b*) we show the four selective wavelength PL images associated with the spectral lines of figure 2(*a*). The images are obtained by integrating the PL emission over the wavelength interval marked in gray on figure 2(*a*). The images are overlaid by a contour plot where each full line represents a 10% change in the emission intensity. The images are numbered in accordance with the spectral domains from figure 2(*a*). These images allow an accurate determination of the spatial source for each spectral feature. The position of the (100)-oriented strained 18, 38, 75 and 150 Å InGaAs QWs is clearly identified by these images. We have marked these positions by the bold broken lines on the images, for later reference.

In figures 3(*a*) and 3(*b*) we show PL spectra and fixed wavelength images for recombination associated with the 80 Å (110)-oriented GaAs/AlGaAs QW for the same scan area as for figure 2. The four broken bold lines of figure 3(*b*) mark the position of the strained (100)-oriented InGaAs QWs as determined from figure 2(*b*). The uppermost spectrum in figure 3(*a*) is dominated by a spectral line which peaks at 793 nm. This PL emission line is typical of the (110)-oriented CEO 80 Å GaAs/AlGaAs QW as verified by far-field spectroscopy in this work and previous studies [3, 7, 8]. This spectrum is from a pixel midway between the 38 and 75 Å strained QW. The image clearly shows that the spatial origin of this emission strongly anticorrelates with the positions of the strained QWs, peaking between them. The lower three spectra in figure 3(*a*) originate from pixels above the three strained QWs. The spectral line marked 2 arises above the 18 Å strained QW and the lines marked 3 and 4 originate above the 75 and 150 Å QWs respectively. The fixed wavelength images of these spectral lines strongly correlate with the spatial position of the (100)-oriented strained InGaAs QWs, as can be seen in figure 3(*b*). There can be no doubt that the strain field of the underlying (100) InGaAs layers perturbs the (110) GaAs QW and shifts its emission to lower energy relative to the emission from the unperturbed QW. This perturbation affects the semiconductor band structure only directly above the strained InGaAs QWs, and thus along a very well defined direction in the (110)-oriented QW plane. This direction defines the SQWR where carriers are confined to narrow stripes within the (110)-oriented GaAs QW plane. The three lower PL spectra in figure 3(*a*) are thus assigned to carrier recombination within the single SQWRs. The magnitude of these shifts, as large as 20 meV for the 150 Å SQWR from both the 80 and 35 Å (110)-

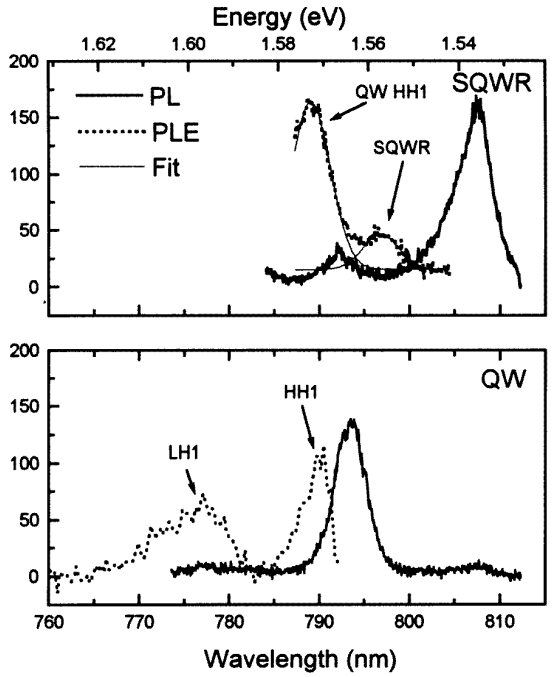

Figure 4. Near-field PL (full curve) and PLE (dotted curve) spectra of the 80 Å (110) QW and the 150 Å × 80 Å SQWR. A two-Gaussians model fit used to determine the relative intensity is shown by the broken line.

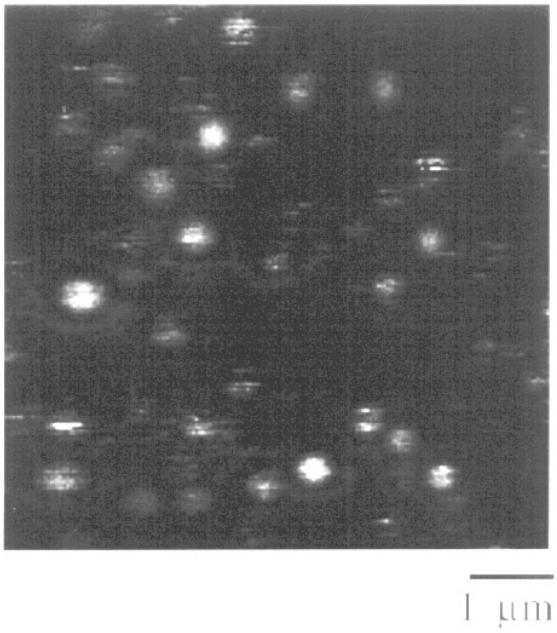

Figure 5. Photoluminescence emission image of 4 nm CdSe crystallites excited at 532 nm. Resolution is determined by the 1.4 NA oil immersion objective used in this scanning confical microscopy image. Detection is with a silicon avalanche photodiode.

oriented QWs (the latter is not discussed in this study), is in agreement with previous measurements using far-field optics and a large array of QWRs [3, 7, 8]. As expected, the magnitude of the shift scales with the width of the strained layer which determines the dimension of the lateral confinement [11]. Another demonstration of the confinement to 1D can be readily seen in the images of figure 3(*b*) and the spectra of figure 3(*a*). We note that both the PL images and the near-field PL spectra (sharp spectral 'spikes') clearly indicate that the emission from both the QWs and QWRs originate from fully (0D) localized centres [12]. It is clearly seen that the near-field PL spectra from the QWRs are broader and have a greater number of sharp spectral lines than that of the QW. This difference obtains from the limitation of carrier diffusion in one of the lateral dimensions.

In figure 4 we show the PL (full curve) and PLE (broken curve) spectra of the 150 Å SQWR and the (110)-oriented 80 Å GaAs QW from a position between the strained (100)-oriented InGaAs QWs. As discussed above, both the excitation and collection are through the NSOM tip. The all near-field PLE spectrum of the (110) CEO GaAs QW is indistinguishable from the far-field PLE spectrum (not shown). We use the similarities to verify that background light originating in the fibre was correctly subtracted. The excitonic transitions associated with the first heavy-hole excitons (HH1) and the first light-hole exciton (LH1) are marked in figure 4. The 5 meV Stokes shift between the HH1 transition measured in PLE and that measured in PL is typical of (110)-oriented QWs [13]. Since the NSOM tip, 3000 Å diameter, is far larger than the SQWR, carrier diffusion from the well to the wire cannot be avoided. Consequently all the spectral features associated with QW absorption are seen in the PLE spectrum of the SQWR. The spectral feature centred at 799 nm in the PLE spectrum of the SQWR is at a lower energy than the QW band edge and thus can only be assigned to SQWR absorption. With a few reasonable assumptions, the data of figure 4 can be used to experimentally test for the first time the prediction of enhanced oscillator strength for QWR structures [14]. We assume that all photogenerated carriers up to a tip radius diffuse to recombine in the SQWR. This assumption is supported by the spectra and images of figure 3. There is negligible emission from the QW when the tip is positioned directly over a QWR. Since the magnitudes of PL emission from the SQWRs and the QW are comparable, non-radiative recombination can be reasonably ignored. Thus the ratio of QW and QWR oscillator strength can be measured by comparing the peak area of the lowest energy transition of the QW to that of the SQWR as observed in the PLE spectrum of the SQWR, correcting for the geometric area of the two structures. The QW to SQWR area ratio under the tip is approximately 20:1, while the QW–QWR PLE intensity ratio is roughly 6:1 as determined by the two-Gaussians model fit to the data shown in figure 4. A factor of three enhancement in the absorption of the wire with respect to that of the well is thus determined. This demonstration of the increase in the QWR oscillator strength is in agreement with theoretical estimations [14].

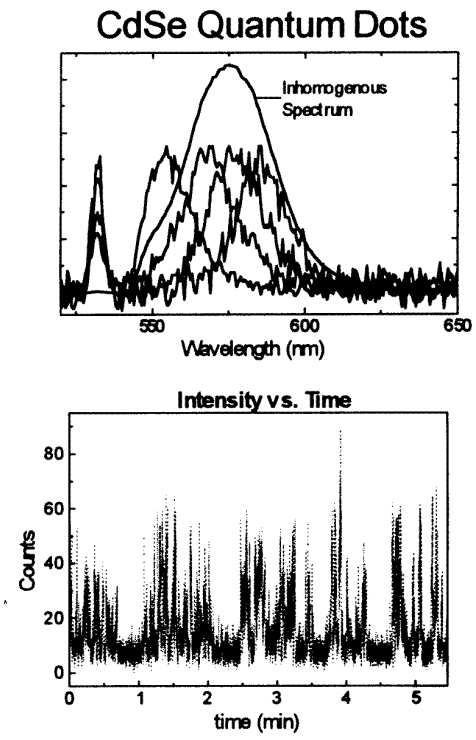

Figure 6. Upper panel: photoluminescence spectra of several particles compared with a spectrum of a large number. Lower panel: sequential time record of photon arrival times for one particle in the image of figure 5. Non-exponential statistics characterize the dynamics at both long and short times.

5. CdSe single quantum dots

Recently, single-molecule characterization has been revolutionized by NSOM and CSOM (confocal scanning optical microscopy) [15–17]. We show here recent room-temperature studies of chemically synthesized CdSe nanocrystals [18]. Heterogeneity has been a particularly difficult barrier to understanding the photophysics of nanocrystals. In figure 5 we show an image of 3.5 nm CdSe nanocrystals dispersed onto a polymer-coated silica cover-slip. Since lateral resolution is $\sim 0.3\ \mu$m, the diffraction limit, coverage is adjusted to give appropriate particle separation. Details of the instrumentation were described previously as were sample preparation procedures [17, 18]. We show here preliminary spectroscopy and dynamics to illustrate the advantage of this experimental strategy. In figure 6 we show representative spectra and photoemission dynamics of one CdSe particle. The PL spectrum line width is typically half the ensemble line width for the best available samples. Even more dramatic is the shift to high energy with time. The most immediate interpretation is that the particle is undergoing photochemistry, probably oxidation, yielding a smaller particle with time. The photochemistry is also reflected in the emission dynamics. The emission time record shows alteration of the trap dynamics. The emission decay time is typically 20 ns. However, there is clear evidence of a long-lived trap state which results in millisecond long 'dark' periods. The nature of the traps is currently under study. Variation of temperature and excitation density will permit determination of both trap energetics and kinetics of state crossing.

This measurement strategy allows unambiguous determination of the effect of surface passivation chemistry. Differentation of trapping probablility versus trap depth and lifetime is greatly simplified by single-particle studies. The observation of simultaneous spectral shifts, not visible for ensembles, and increased trapping times reveals that chemical evolution is the primary avenue for particle stabilization. Repetition of the measurement in inert atmospheres will immediately reveal the role of internal chemical stability.

6. Conclusion

Using NSOM spectroscopy, we produced photoluminescence and photoluminescence excitation spectra of single quantum wires for the first time. The spatial position of strained, cleaved edge overgrown (110) quantum wires is coincident with the underlying strained (100) quantum wells, and the magnitude of the SQWR energy shift scales with this (100) QW width. From the near-field PLE spectrum we estimate a factor of three oscillator strength enhancement for this semiconductor quantum wire relative to a comparable QW. Using room-temperature scanning confocal microscopy we are able to study the excited state decay dynamics of single nanometre dimension CdSe crystallites. Unique insight is gained for measurements of single entities compared to ensembles.

References

[1] Arakawa Y and Sakaki H 1982 *Appl. Phys. Lett.* **40** 939
Arakawa Y, Vahala K and Yariv A 1984 *Appl. Phys. Lett.* **45** 950
[2] Pfeiffer L N, West K W, Stormer H L, Eisenstein J, Baldwin K W, Gershoni D and Spector J 1990 *Appl. Phys. Lett.* **56** 1697
[3] Gershoni D, Weiner J S, Chu S N G, Baraff G A, Vandenberg J M, Pfeiffer L N, West K W, Logan R A and Tanbun-Ek T 1990 *Phys. Rev. Lett.* **65** 1631
[4] Goni A R, Pfeiffer L N, West K W, Pinzuck A, Baranger H U and Stormer H L 1992 *Appl. Phys. Lett.* **61** 1956
[5] Dingle R, Wiegmann W and Henry C H 1974 *Phys. Rev. Lett.* **33** 827
[6] Wegscheider W, Pfeiffer L N, Dignam M M, Pinczuk A, West K W, McCall S L and Hull R 1993 *Phys. Rev. Lett.* **71** 4071
[7] Gershoni D, Katz M, Wegscheider W, Pfeiffer L N, Logan R A and West K W 1994 *Phys. Rev.* B **50** 8930
[8] Gershoni D, Weiner J S, Fitzgerald E A, Pfeiffer L N and Chand N 1993 *Optical Phenomena in Semiconductor Structures of Reduced Dimensions* ed D J Lockwood and A Pinczuk (Dodrecht: Kluwer) p 337
[9] Grober R D, Harris T D, Trautman J K and Betzig E 1994 *Rev. Sci. Instrum.* **65** 626
[10] Grober R D, Harris T D, Harris J K, Betzig E, Wegscheider W, Pfeiffer L and West K 1994 *Appl. Phys. Lett.* **64** 1421
[11] Baraff G A and Gershoni D 1991 *Phys. Rev.* B **43** 4011
[12] Hess H F, Betzig E, Harris T D, Pfeiffer L N and West K W 1994 *Science* **264** 1740
[13] Gershoni D, Brener I, Baraff G A, Chu S N G, Pfeiffer L N and West K 1991 *Phys. Rev.* B **44** 1931

[14] Suemune I and Coldren L A 1988 *IEEE J. Quantum Electron.* **24** 1778
[15] Betzig E and Chichester R 1993 *Science* **262** 1422
[16] Trautman J K, Macklin J J, Brus L E and Betzig E 1994 *Nature* **369** 40
[17] Macklin J J, Trautman J K, Harris T D and Brus L E 1996 *Science* **272** 255
[18] Murray C B, Norris D J and Bawendi M G 1993 *J. Am. Chem. Soc.* **115** 8706